The glass transition of water, insight from phase change materials.

Pierre Lucas[1,*], Julian Pries[2], Shuai Wei[3], Matthias Wuttig[2,4]

[1]Department of Materials Science and Engineering, University of Arizona, Tucson, AZ, 85712, USA
[2]Institute of Physics IA, RWTH Aachen University, 52074 Aachen, Germany
[3]Department of Chemistry and iMAT, Aarhus University, DK-8000 Aarhus-C, Denmark
[4]Peter Grünberg Institute (PGI 10), Forschungszentrum Jülich, 52428 Jülich, Germany
[*] *E-mail address:* pierre@ arizona.edu.

Abstract: The calorimetric features that have been broadly used to assign a glass transition temperature T_g of 136 K to amorphous water are qualitatively reproduced with a phase change material. Annealing treatments and ultrafast calorimetry measurements indicate that this feature is only a shadow-T_g and that the real T_g lies at higher temperature above the glass transition. A Kissinger analysis of the crystallization kinetics confirms that crystallization occurs below T_g from the glassy state at conventional heating rates. These results strongly suggest that the amorphous water endotherm at 136 K is indeed a shadow-T_g and that the real T_g lies at higher temperature as predicted from structural relaxation considerations.

Introduction

Water may be regarded as the most important molecules on earth for its role in creating and sustaining life. Water on earth is found in the liquid and crystalline ice form, yet the majority of water in the universe exists in the amorphous state on the surface of interstellar grains[1]. The first artificial form of amorphous water was produced in 1935 by vapor deposition[2], yet to this day, one of the most essential property of amorphous water: its glass transition temperature, remains unclear. Amorphous water can be obtained in several forms depending on the preparation method[3]. Amorphous water is produced by compression of ice I_h to obtain the high-density amorphous form (HDA)[4]. This HDA form can subsequently be converted to the low-density amorphous form (LDA) by reheating at ambient pressure. Another form commonly called amorphous solid water (ASW) can be produced by vapor deposition and is present on interstellar dust particles[1]. ASW can also be produced and studied in the laboratory by depositing vapor on a Cu substrate precooled at 77 K[5]. Finally hyperquenched glassy water (HGW) is produced by cooling suspended droplets of liquid water projected at supersonic speed on a Cu substrate precooled at 77 K[6]. Whether these forms of amorphous water can be formally regarded as vitreous depends on whether they exhibit a measurable glass transition. In that respect, the topic of the glass transition of water has been mired in controversy for more than four decades[7-14]. A value of 136 K for the glass transition temperature T_g of water has been broadly accepted based on direct calorimetric measurements of annealed HGW[6]. This value was also found to be consistent with T_g extrapolation of binary aqueous solutions[7]. However, it was later argued that the correct T_g should be closer to 165 K based on the measurement of pre-T_g exotherms for multiple hyperquenched glasses[10]. It was then concluded that the T_g of amorphous water cannot be directly measured due to fast crystallization during heating at conventional rates near 20 K/min. It was further argued that the endotherm observed at 136 K is instead a shadow-T_g resulting from the prior annealing procedure[11]. This was consistent with the observation that the magnitude of the faint endotherm at 136 K is only a fraction of what is expected for the heat

capacity jump at the glass transition of water[7]. Other models have invoked non-equilibrium correlation lengths as the source of the endotherm at 136 K[12].

Water shares many unusual properties with phase change materials. Both are thought to undergo a liquid-liquid phase transition[13,15,16], both are thought to undergo a fragile-to-strong transition[17,18] and both exhibit a breakdown of the Stokes-Einstein relation near the melting point[19]. In this study, we compare the calorimetric signature of ASW with that of the phase change material (PCM) $Ge_2Sb_2Te_5$ (GST) and show that they exhibit qualitatively similar behavior. Both samples crystalize without exhibiting a calorimetric glass transition unless they are previously annealed and both develop a pre-crystallization endotherm upon annealing. But in the case of GST, ultrafast calorimetry measurements unambiguously show that the observed endotherm prior to crystallization is indeed a shadow-T_g and that the real T_g lies at much higher temperature. This conclusion is further corroborated by a Kissinger analysis of the crystallization kinetics. The shadow-T_g is a natural feature of annealed hyperquenched glasses resulting from the spectrum of relaxation times present in all amorphous solids. The similarity between water and GST therefore provides support for the conclusion that the correct T_g for water should be higher than 136 K as previously suggested[10,11].

Experiment

Joari and coworker have shown that the structures and calorimetric signatures of ASW and HGW are almost indistinguishable[5]. Amorphous phase change materials (PCMs) can also be produced in the same two ways, either by hyperquenching or by physical vapor deposition, but it is very challenging to produce sufficiently large samples by hyperquenching for calorimetric measurements. This is because the laser-assist hyperquenching can only melt a small area (~a few micrometer in diameter) of thin film samples of PCMs. In this work we therefore produce GST samples by physical vapor deposition as previously described[20]. The resulting GST films were about 4 μm thick and were easily peeled off the substrate for calorimetric measurements. Standard and ultrafast differential scanning calorimetry (DSC) were used to characterize the samples after different heat treatments. Standard DSC was performed at a heating rate of 40ºC/min with a Q1000 from TA Instrument using hermetic T-zero pans containing about 10 mg of GST flakes. An empty pan was used as a reference. Temperature was calibrated with an indium standard and heat flow was calibrated with a sapphire standard. Ultrafast DSC was performed as previously described[20]. The excess heat capacity was calculated by subtracting the crystal thermogram obtained directly after crystallization, from the glass thermogram.

Result and Discussion

PCMs are by design extremely poor glass formers because conversion between the amorphous and crystalline phase should happen in the nanosecond regime to unable fast memory and computing applications[21]. In fact PCMs such as GST are such poor glass former that they do not exhibit a calorimetric glass transition upon reheating at conventional rates (in the range of tens of degrees per minute). As shown in Fig. 1, GST shares this particularity with water. Instead of a glass transition, both GST and HGW exhibit a notable exotherm prior to the crystallization peak. This exotherm is a well-known consequence of non-linear relaxation in glassy solids[22,23].

Because poor glass formers can only be obtained at very high effective cooling rates, they are trapped in a high fictive temperature and high configurational entropy state. Following the TNM equation[24] or the Adam-Gibbs equation[25], the structural relaxation time of these glasses is therefore considerably shorter than that of slow-cooled glasses. In particular, the relaxation time of hyperquenched glasses is shorter than the characteristic time during reheating in the DSC at conventional rates. As a result, the structure can start relaxing exothermically towards the metastable liquid state while the glass is still heating towards the glass transition. This gives rise to the exotherms in Fig 1a&b which is eventually interrupted by crystallization before the glass transition can be observed.

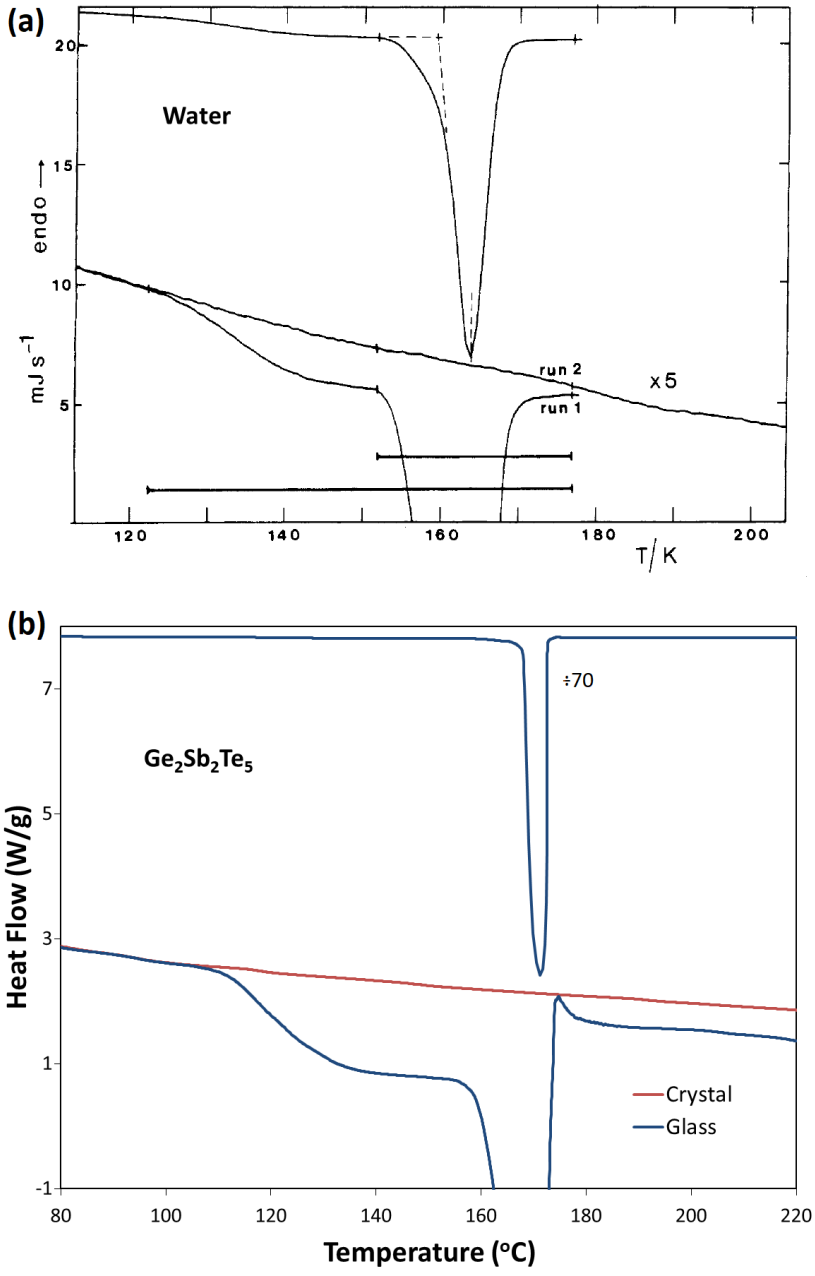

Fig 1: (a) Thermogram of a vitrified liquid water sample (HGW). Lower curve is the same data with ordinate fivefold expanded. Run 1 is the HGW and run 2 is the same sample after crystallization into ice. Reprinted with permission from Ref [26]. Copyright 1987 American Chemical Society; (b) Thermogram of amorphous $Ge_2Sb_2Te_5$ and the same sample after crystallization. The upper curve is the glass thermogram reduced 70 times.

In an effort to circumvent this effect, prior studies have relied on pre-annealing procedures to release the trapped enthalpy and observe the glass transition of hyperquenched samples[5,6,27]. HGW and ASW were annealed at 130K for 90 min[5,6], i.e. 6K below the subsequent pre-T_g endotherm, while GST was annealed at 114ºC for 37 h[27], i.e. 35K below the subsequent pre-T_g endotherm. However, the assignment of these pre-T_g endotherms as the correct T_g for water and GST has since then been questioned[11,20].

According to the TNM model[24], release of the trapped enthalpy during annealing should depend on both time and temperature. The effects of annealing time and temperature on amorphous GST are illustrated in Fig 2. The effect of time is illustrated in Fig. 2a where the exotherm is found to progressively disappear during isothermal heat treatment at 90ºC. The effect of temperature is illustrated in Fig. 2b where the exotherm disappears more rapidly at high temperature during isochronal heat-treatments. This is consistent with the expectation that the structural relaxation time is shorter at higher temperature. In either case, the hyperquenched glass releases increasing amounts of trapped enthalpy and its fictive temperature decreases towards the standard T_g (i.e. T_g measured at standard heating rate). At that point the relaxation time has increased sufficiently that the sample cannot relax exothermically during standard heating. The exotherm is therefore removed. But upon further heat-treatment at sufficiently high temperature or for sufficiently long time, a shallow endothermic peak eventually forms just prior to crystallization. The magnitude of this endotherm is much smaller than expected for a normal glass transition, but it has commonly been associated with the onset of a glass transition that would be partially masked by crystallization[5,6,27]. Below, we show that it is actually a pre- T_g endotherm known as shadow- T_g that is a normal consequence of annealing in hyperquenched glasses.

The long standing debates regarding the T_g of water and GST stems from the fact that crystallization obscures most of the glass transition. Hence, in order to clarify the nature of the endotherm, it is informative to examine the behavior of a good glass former that is entirely devoid of crystallization upon reheating at standard rates. The case of a telluride glass with a T_g in a similar range as GST but with excellent glass-forming ability is shown in Fig. 3. This glass was quenched during fiber drawing at a rate estimated at ~500ºC/min. As discussed above, structural relaxation depends on both temperature and time, and in this case the annealing temperature was very low (room temperature i.e. 110K below T_g) but the annealing time was extensive, up to 60 months. The thermograms of Fig. 3 initially show the characteristic exotherm associated with quenched glasses, as in Fig. 1 for GST and HGW. But upon longer annealing, a pre- T_g endotherm clearly develops over time. If a T_g value were to be extracted from this endotherm it would yield 100ºC which is more than 30 degrees lower than the actual T_g = 132ºC for $Te_2As_3Se_5$[28]. Similar behaviors have been widely observed in metallic glasses[29,30]. This peculiar endotherm is a well-known consequence of non-exponential relaxation in glassy

solids[22,23]. All glasses have a spectrum of relaxation times equivalent to a distribution of local fictive temperatures. Annealing below T_g selectively relaxes the glass components with shorter relaxation times. Upon subsequent reheating these same components collectively regain enthalpy to give rise to the shadow-T_g observed in Fig. 3. The same behavior is expected for water and GST as it is a universal feature resulting from the spectrum of relaxation times intrinsic to glasses. This process only involves a small fraction of the glass and also explains the shallow nature of the endotherm observed in both HGW and GST. The actual glass transition for the remaining bulk of the sample then occurs at higher temperature as evidenced in Fig. 3 but is hidden by crystallization in the case of HGW and GST.

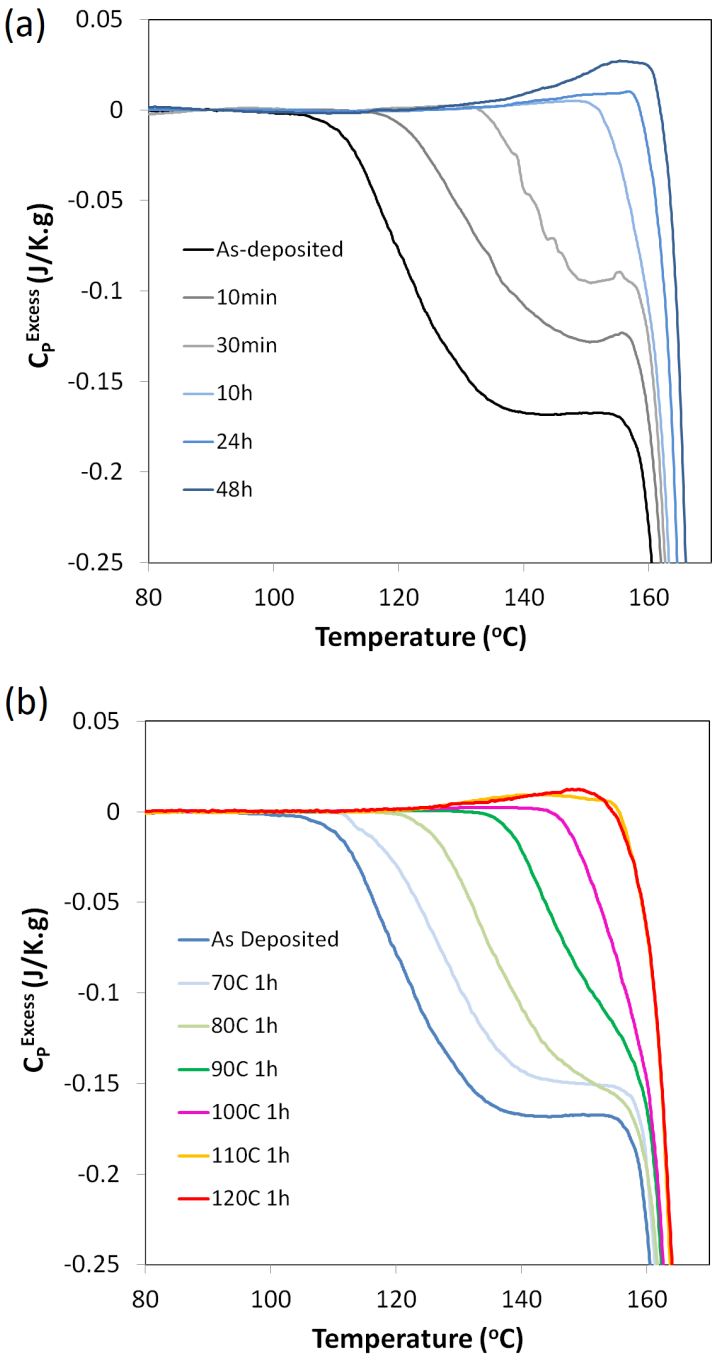

Fig 2: (a) Excess heat capacity of amorphous $Ge_2Sb_2Te_5$ after isothermal heat-treatment at 90ºC for increasing time lengths; (b) Excess heat capacity of amorphous $Ge_2Sb_2Te_5$ after isochronal heat-treatment for 1 h at increasing temperature (data taken from Ref [20]).

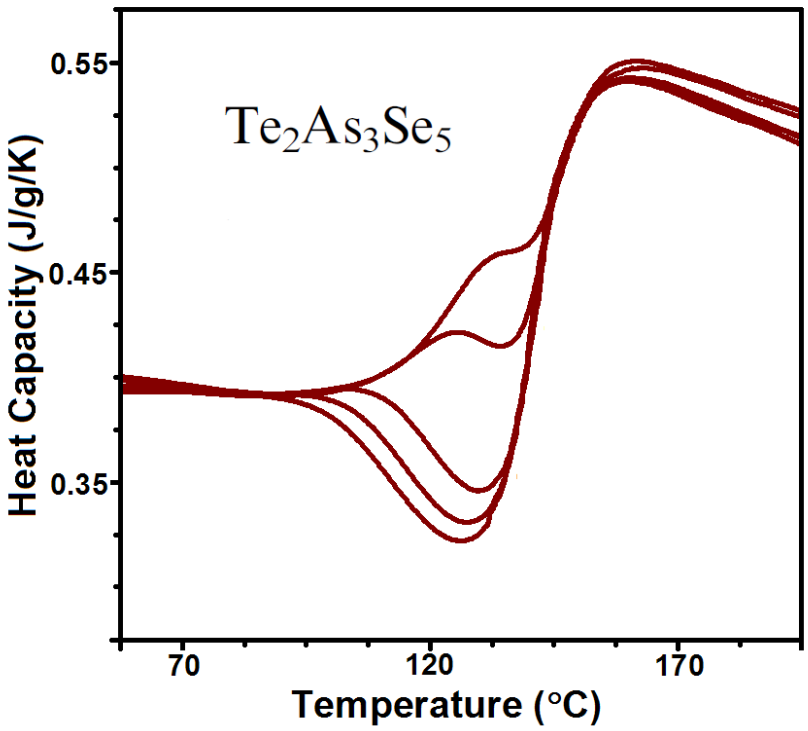

Fig 3: Thermogram of amorphous $Te_2As_3Se_5$ glass fibers quenched at ~500ºC/min and annealed at room temperature for 1 week, 1 month, 4 months, 19 months and 60 months (in order of disappearing exotherm). A pre-T_g endotherm develops upon annealing. The onset of that endotherm is about 30ºC lower than the actual T_g.

As discussed above, the exotherm of hyperquenched glasses is merely the consequence of fast structural relaxation times relative to the heating rate. No exotherm is expected if the heating rate is the same as the effective cooling rate. Hence, another way of circumventing the exotherm to reveal the glass transition is to increase the heating rate. However, this can be experimentally challenging for samples quenched at extreme rates. Nevertheless, it is accessible using ultrafast DSC in the case of phase change materials[20,31]. The excess heat capacity of GST during heating at rates spanning three orders of magnitudes is shown in Fig. 4. As expected, a deep exotherm is observed at the lowest heating rates. But the exotherm progressively disappears as the heating rate increases. The pre-T_g endotherm also develops concomitantly even as the relaxation exotherm is still present prior to crystallization (3500 - 7,500 K/s). This is a clear indication that the endotherm does not correspond to the real glass transition. Eventually the heating rate is sufficiently high (>10,000 K/s) to prevent any exothermic relaxation and the thermogram exhibits a single glass transition onset with no prior exotherm (and no prior annealing). This endotherm can then be considered to be the real glass transition for this given heating rate. For GST, the thermograms start exhibiting a single glass transition for cooling rates near 10,000 K/s. This implies that the effective cooling rate for that sample should be in the same range. This is consistent with effective cooling rates estimated for similar sputtered telluride films[32]. The

standard T_g at a rate of 20 K/min can then be derived from Moynihan's method using equation 1[33,34].

$$log\frac{Q}{Q_s} = m \cdot \left(1 - \frac{T_g^s}{T_g}\right) \quad (1)$$

where Q is the heating rate, Q_s is the standard heating rate of 20 K/min, T_g^s is the standard T_g and m is the fragility index ~90 for GST[35]. A measured T_g near 220 ºC at 20,000K/s yields a standard T_g^s near 200 ºC. This value is consistent with that derived from exothermic relaxation considerations[20]. This value of T_g^s however, is roughly 70ºC higher than the onset of the endotherm in Fig 2. This clearly indicates that the endotherm does not correspond to the real glass transition. Similarly, the T_g of 136 K derived from the endotherm for water[6] is nearly 30 K lower than that of 165 K derived from exothermic relaxation considerations[10]. This exemplifies the potential for error of using annealed samples to derive T_g of hyperquenched glasses with a strong propensity for crystallization.

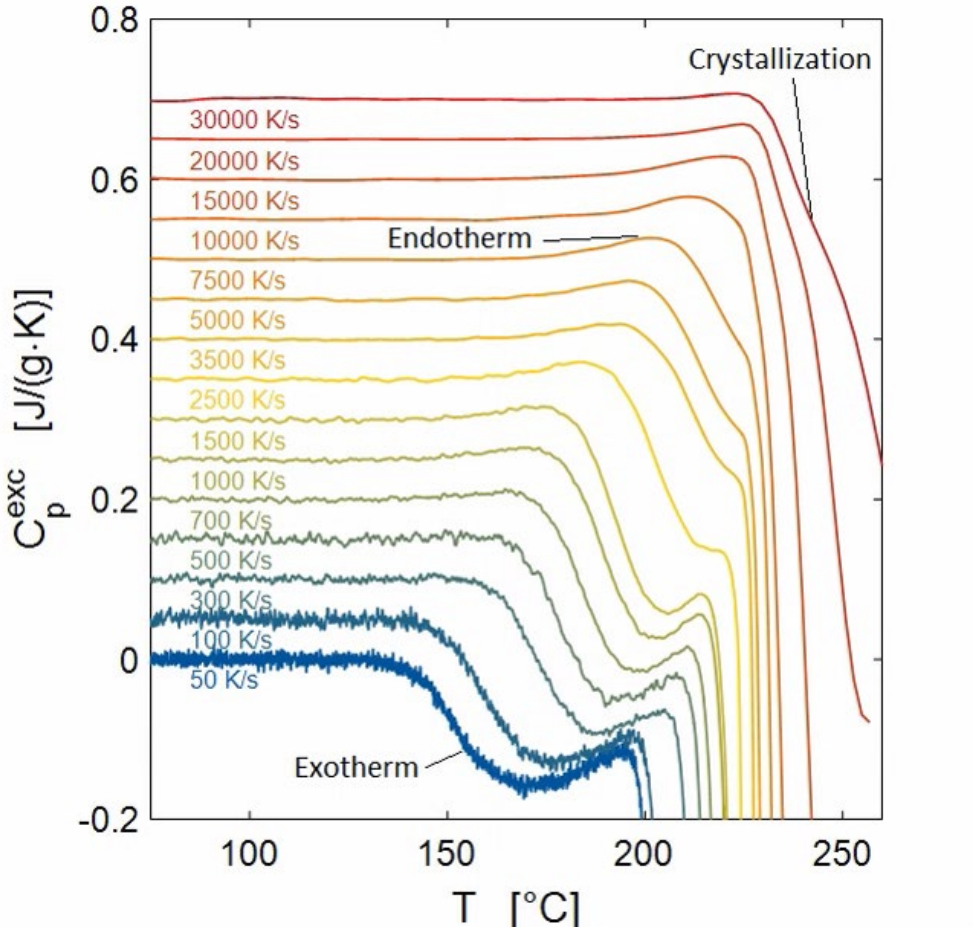

Fig. 4: Ultrafast DSC thermogram of amorphous $Ge_2Sb_2Te_5$ at heating rates of 100 K/s to 30,000K/s. (data taken from Ref [20]).

These results also signify that both GST and water must crystallize below T_g (from the glassy state) when reheated at conventional rates. Fig. 4 shows that GST crystallizes below T_g for heating rates lower than 10,000 K/s. For greater heating rates, the crystallization exotherm occurs above T_g. The kinetics of crystallization are therefore expected to be different in each conditions, since in one case crystallization occurs from the solid state, and in the other case it occurs from the supercooled liquid state. Interestingly, the kinetics of crystallization can be investigated by performing a Kissinger analysis of the thermograms from Fig. 4. As expected from the Kissinger model[36] the maximum crystallization temperature T_c shifts to higher temperature with increasing heating rates (Fig. 5a). The activation energy for crystallization E_k can then be derived by building a Kissinger plot according to equation 2[36,37]:

$$ln\left(\frac{Q}{T_c^2}\right) = \frac{E_k}{k_B T_c} + ln\left(K_o \frac{k_B}{E_k}\right) \quad (2)$$

where k_B is the Boltzmann constant and K_o is a constant. Such a plot is shown in Fig. 5b including both ultrafast and standard DSC data covering a heating rate range of nearly seven orders of magnitude. The most striking feature from this plot is a sudden change in activation energy starting at heating rates > 10,000 K/s. This change in E_k is a clear indication that the crystallization kinetics switch between two different regimes. This observation is in turn fully consistent with the conclusion derived from Fig. 4. For heating rates lower than 10,000 K/s GST crystallizes from the glassy state, while at higher rates it crystalizes from the supercooled liquid state. Fig. 1 and 2 were collected at 40 K/min hence this confirms that GST crystallizes from the glassy state in theses thermograms. This in turns confirms that the endotherm observed upon annealing is not the real glass transition. This behavior appears to be generalized among PCMs as it has also been observed in AgInSbTe samples[31].

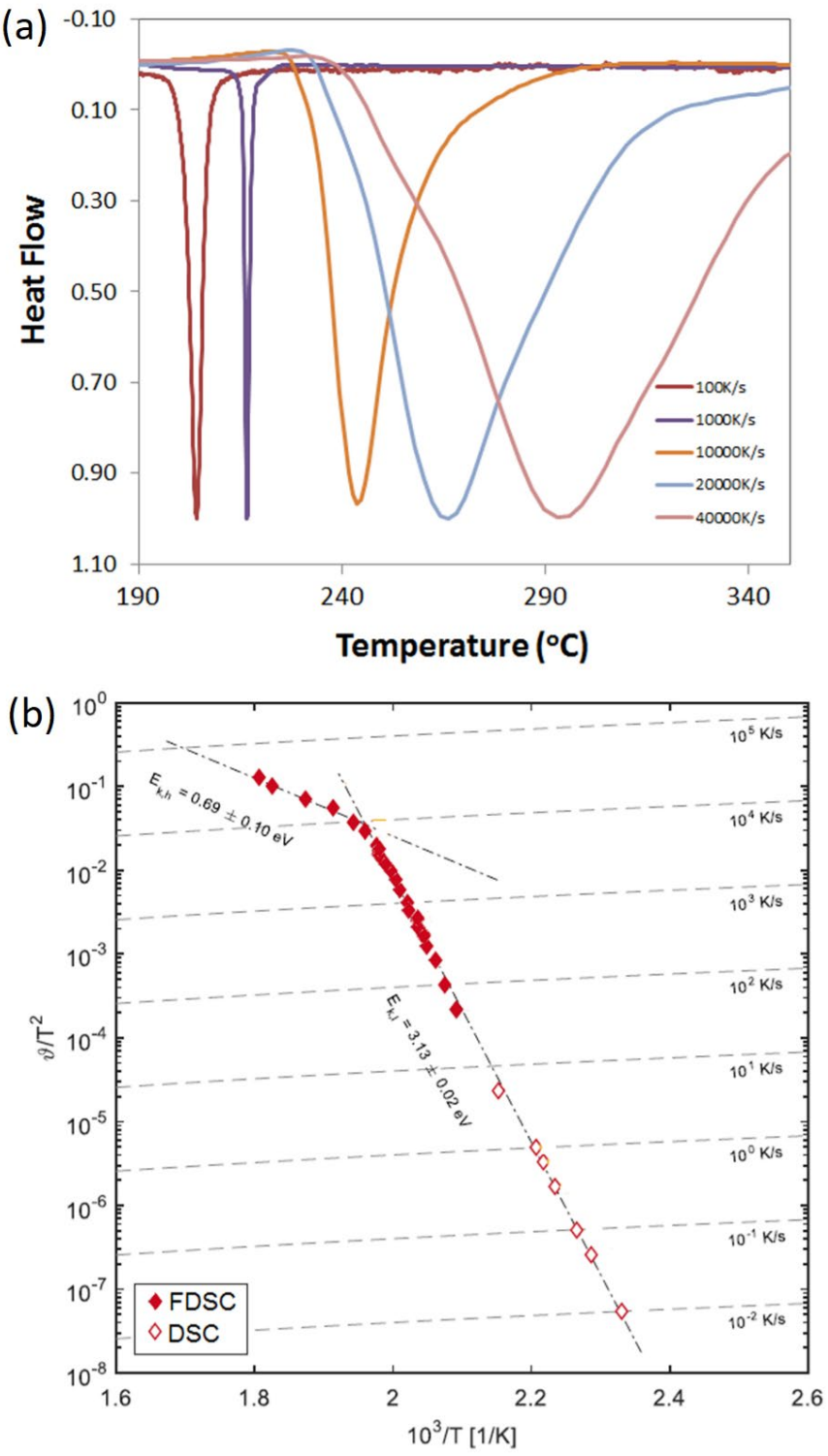

Fig. 5: (a) Crystallization exotherm of amorphous $Ge_2Sb_2Te_5$ measured at heating rates of 100 K/s to 40,000K/s; (b) Kissinger plot of $Ge_2Sb_2Te_5$ based on standard and ultrafast DSC thermograms spanning nearly seven order in magnitude in heating rates. (data taken from Ref [20]).

Conclusion

Amorphous PCMs and amorphous water share many unusual properties. The PCM $Ge_2Sb_2Te_5$ is therefore used to draw analogy for the thermal behavior of water. It is found that the pre-crystallization endotherm developing upon annealing is not the actual glass transition but only a shadow-T_g resulting from the broad spectrum of relaxation times intrinsic to glassy solids. This assignment is confirmed by comparison with a good glass-former subjected to extensive annealing. The real glass transition is then unambiguously measured by ultrafast DSC. A Kissinger analysis confirms that the PCM crystallizes from the glassy state at low heating rates. The universal nature of non-exponential relaxation in glass strongly suggests that the pre-crystallization endotherm observed in annealed amorphous water is also a shadow-T_g. It is then suggested that ultrafast DSC applied to amorphous water should enable a direct measurement of the correct T_g for amorphous water. This could help settle a long-standing scientific dispute. Yet, this does not answer all questions. We should also further our understanding which materials are bad glass formers with rather low reduced glass transitions temperatures (T_g/T_m). For phase change materials, it has been possible to relate the reduced glass transition temperature with quantum chemical bonding descriptors in the crystalline state[38]. These quantities apparently help to understand and predict material properties[39], as well as the crystallization and vitrification of a group of chalcogenides employed in phase change materials. These materials are characterized by an unconventional bonding mechanism in the crystalline state, called metavalent bonding[40]. It is characterized by the formation of half an electron pair between two atoms (also described as sharing one electron between two atoms), i.e. a bond order of ½. This unique bonding mechanism explains many of the unconventional properties of phase change materials[41,42]. It is tempting to speculate how bonding may play a role in the origin of the vitrification of water and its solutions.

Acknowledgment

We would like to express our deepest gratitude to Austen Angell to whom this paper is dedicated. Through his enthusiasm and enlightening conversations Austen provided the inspiration for this study and many others. His energy and passion for science will be greatly missed. PL acknowledges funding from NSF-DMR grant#: 1832817.

References

1 Mayer, E. & Pletzer, R. Astrophysical implications of amorphous ice—a microporous solid. *Nature* **319**, 298-301, (1986), doi:10.1038/319298a0.

2 Burton, E. F. & Oliver, W. F. X-Ray Diffraction Patterns of Ice. *Nature* **135**, 505-506, (1935), doi:10.1038/135505b0.

3 Angell, C. A. AMORPHOUS WATER. *Annual Review of Physical Chemistry* **55**, 559-583, (2004), doi:10.1146/annurev.physchem.55.091602.094156.

4 Mishima, O., Calvert, L. D. & Whalley, E. 'Melting ice' I at 77 K and 10 kbar: a new method of making amorphous solids. *Nature* **310**, 393-395, (1984), doi:10.1038/310393a0.

5 Hallbrucker, A., Mayer, E. & Johari, G. P. Glass-liquid transition and the enthalpy of devitrification of annealed vapor-deposited amorphous solid water: a comparison with

hyperquenched glassy water. *The Journal of Physical Chemistry* **93**, 4986-4990, (1989), doi:10.1021/j100349a061.
6 Johari, G. P., Hallbrucker, A. & Mayer, E. The glass–liquid transition of hyperquenched water. *Nature* **330**, 552-553, (1987), doi:10.1038/330552a0.
7 Angell, C. A. Liquid Fragility and the Glass Transition in Water and Aqueous Solutions. *Chemical Reviews* **102**, 2627-2650, (2002), doi:10.1021/cr000689q.
8 Johari, G. P. Does water need a new Tg? *The Journal of Chemical Physics* **116**, 8067-8073, (2002), doi:10.1063/1.1466469.
9 Johari, G. P., Hallbrucker, A. & Mayer, E. Two Calorimetrically Distinct States of Liquid Water Below 150 Kelvin. *Science* **273**, 90-92, (1996), doi:10.1126/science.273.5271.90.
10 Velikov, V., Borick, S. & Angell, C. A. The glass transition of water, based on hyperquenching experiments. *Science* **294**, 2335-8, (2001).
11 Yue, Y. & Angell, C. A. Clarifying the glass-transition behaviour of water by comparison with hyperquenched inorganic glasses. *Nature* **427**, 717-20, (2004).
12 Limmer, D. T. & Chandler, D. Theory of amorphous ices. *Proceedings of the National Academy of Sciences*, 201407277, (2014), doi:10.1073/pnas.1407277111.
13 Angell, C. A. Insights into Phases of Liquid Water from Study of Its Unusual Glass-Forming Properties. *Science* **319**, 582, (2008), doi:10.1126/science.1131939.
14 Amann-Winkel, K., Gainaru, C., Handle, P. H., Seidl, M., Nelson, H., Böhmer, R. & Loerting, T. Water's second glass transition. *Proceedings of the National Academy of Sciences* **110**, 17720, (2013), doi:10.1073/pnas.1311718110.
15 Zalden, P., Quirin, F., Schumacher, M., Siegel, J., Wei, S., Koc, A., Nicoul, M., Trigo, M., Andreasson, P., Enquist, H., Shu, M. J., Pardini, T., Chollet, M., Zhu, D., Lemke, H., Ronneberger, I., Larsson, J., Lindenberg, A. M., Fischer, H. E., Hau-Riege, S., Reis, D. A., Mazzarello, R., Wuttig, M. & Sokolowski-Tinten, K. Femtosecond x-ray diffraction reveals a liquid–liquid phase transition in phase-change materials. *Science* **364**, 1062, (2019), doi:10.1126/science.aaw1773.
16 Wei, S., Lucas, P. & Angell, C. A. Phase-change materials: The view from the liquid phase and the metallicity parameter. *MRS Bulletin* **44**, 691-698, (2019), doi:10.1557/mrs.2019.207.
17 Ito, K., Moynihan, C. T. & Angell, C. A. Thermodynamic determination of fragility in liquids and a fragile-to-strong liquid transition in water. *Nature* **398**, 492-495, (1999), doi:10.1038/19042.
18 Wei, S., Lucas, P. & Angell, C. A. Phase change alloy viscosities down to Tg using Adam-Gibbs-equation fittings to excess entropy data: A fragile-to-strong transition. *J. Appl. Phys.* **118**, 034903/1-034903/9, (2015), doi:10.1063/1.4926791.
19 Wei, S., Evenson, Z., Stolpe, M., Lucas, P. & Angell, C. A. Breakdown of the Stokes-Einstein relation above the melting temperature in a liquid phase-change material. *Science Advances* **4**, 8632, (2018).
20 Pries, J., Wei, S., Wuttig, M. & Lucas, P. Switching between Crystallization from the Glassy and the Undercooled Liquid Phase in Phase Change Material Ge2Sb2Te5. *Advanced Materials*, 1900784, (2019), doi:10.1002/adma.201900784.
21 Loke, D., Lee, T. H., Wang, W. J., Shi, L. P., Zhao, R., Yeo, Y. C., Chong, T. C. & Elliott, S. R. Breaking the Speed Limits of Phase-Change Memory. *Science (Washington, DC, U. S.)* **336**, 1566-1569, (2012), doi:10.1126/science.1221561.
22 I. M. Hodge & Berens, A. R. Effects of annealing and prior history on enthalpy relaxation in glassy polymers. 2. Mathematical modeling. *Macromolecules* **15**, 762, (1982).
23 Hornboll, L., Knusen, T., Yue, Y. & Guo, X. Heterogeneous enthalpy relaxation in glasses far from equilibrium. *Chem. Phys. Lett.* **494**, 37-40, (2010), doi:10.1016/j.cplett.2010.05.077.
24 Moynihan, C. T. Structural relaxation and the glass transition. *Rev. Mineral.* **32**, 1-19, (1995).
25 Adam, G. & Gibbs, J. H. On the Temperature Dependence of Cooperative Relaxation Properties in Glass-Forming Liquids. *The Journal of Chemical Physics* **43**, 139-146, (1965), doi:10.1063/1.1696442.

26 Hallbrucker, A. & Mayer, E. Calorimetric study of the vitrified liquid water to cubic ice phase transition. *The Journal of Physical Chemistry* **91**, 503-505, (1987), doi:10.1021/j100287a002.

27 J.A. Kalb, M. Wuttig & Spaepen, F. Calorimetric measurements of structural relaxation and glass transition temperatures in sputtered films of amorphous Te alloys used for phase change recording. *J. Mat. Res* **22**, 748-754, (2007).

28 Lucas, P., King, E. A., Gueguen, Y., Sangleboeuf, J.-C., Keryvin, V., Erdmann, R. G., Delaizir, G., Boussard-Pledel, C., Bureau, B., Zhang, X.-H. & Rouxel, T. Correlation between thermal and mechanical relaxation in chalcogenide glass fibers. *J. Am. Ceram. Soc.* **92**, 1986-1992, (2009), doi:10.1111/j.1551-2916.2009.03150.x.

29 Hu, L., Zhou, C., Zhang, C. & Yue, Y. Thermodynamic anomaly of the sub-Tg relaxation in hyperquenched metallic glasses. *The Journal of Chemical Physics* **138**, 174508, (2013), doi:10.1063/1.4803136.

30 Chen, H. L. S., Inoue, A. S. & Masumoto, T. Two-stage enthalpy relaxation behaviour of (Fe0.5Ni0.5)83P17 and (Fe0.5Ni0.5)83B17 amorphous alloys upon annealing. *Journal of Materials Science* **20**, 2417-2438, (1985).

31 Pries, J., Sehringer, J. C., Wei, S., Lucas, P. & Wuttig, M. Glass transition of the phase change material AIST and its impact on crystallization. *Materials Science in Semiconductor Processing* **134**, 105990, (2021), doi:https://doi.org/10.1016/j.mssp.2021.105990.

32 Pries, J., Wei, S., Hoff, F., Lucas, P. & Wuttig, M. Control of effective cooling rate upon magnetron sputter deposition of glassy Ge15Te85. *Scripta Materialia* **178**, 223-226, (2020), doi:https://doi.org/10.1016/j.scriptamat.2019.11.024.

33 Moynihan, C. T., Lee, S. K., Tatsumisago, M. & Minami, T. Estimation of activation energies for structural relaxation and viscous flow from DTA and DSC experiments. *Thermochim. Acta* **280/281**, 153-162, (1996), doi:10.1016/0040-6031(95)02781-5.

34 Wang, L.-M., Velikov, V. & Angell, C. A. Direct determination of kinetic fragility indices of glassforming liquids by differential scanning calorimetry: kinetic versus thermodynamic fragilities. *J. Chem. Phys.* **117**, 10184-10192, (2002), doi:10.1063/1.1517607.

35 Orava, J., Greer, A. L., Gholipour, B., Hewak, D. W. & Smith, C. E. Characterization of supercooled liquid Ge2Sb2Te5 and its crystallization by ultrafast-heating calorimetry. *Nat. Mater.* **11**, 279-283, (2012), doi:10.1038/nmat3275.

36 Kissinger, H. E. Reaction Kinetics in Differential Thermal Analysis. *Analytical Chemistry* **29**, 1702-1706, (1957), doi:10.1021/ac60131a045.

37 Blaine, R. L. & Kissinger, H. E. Homer Kissinger and the Kissinger equation. *Thermochimica Acta* **540**, 1-6, (2012), doi:https://doi.org/10.1016/j.tca.2012.04.008.

38 Persch, C., Müller, M. J., Yadav, A., Pries, J., Honné, N., Kerres, P., Wei, S., Tanaka, H., Fantini, P., Varesi, E., Pellizzer, F. & Wuttig, M. The potential of chemical bonding to design crystallization and vitrification kinetics. *Nature Communications* **12**, 4978, (2021), doi:10.1038/s41467-021-25258-3.

39 Raty, J.-Y., Schumacher, M., Golub, P., Deringer, V. L., Gatti, C. & Wuttig, M. A Quantum-Mechanical Map for Bonding and Properties in Solids. *Advanced Materials* **31**, 1806280, (2019), doi:10.1002/adma.201806280.

40 Wuttig, M., Deringer, V. L., Gonze, X., Bichara, C. & Raty, J.-Y. Incipient Metals: Functional Materials with a Unique Bonding Mechanism. *Advanced Materials* **30**, 1803777, (2018), doi:https://doi.org/10.1002/adma.201803777.

41 Kooi, B. J. & Wuttig, M. Chalcogenides by Design: Functionality through Metavalent Bonding and Confinement. *Advanced Materials* **32**, 1908302, (2020), doi:https://doi.org/10.1002/adma.201908302.

42 Zhu, M., Cojocaru-Mirédin, O., Mio, A. M., Keutgen, J., Küpers, M., Yu, Y., Cho, J.-Y., Dronskowski, R. & Wuttig, M. Unique Bond Breaking in Crystalline Phase Change Materials and the Quest for Metavalent Bonding. *Advanced Materials* **30**, 1706735, (2018), doi:10.1002/adma.201706735.